Prediction and Evaluation of Entrainment Processes of Intermittent Gas Jets

A.Kido, T.Sano, H.Ogawa and N.Miyamoto

Department of Mechanical Engineering
Hokkaido University
N-13, W-8, Kita-ku, Sapporo 060
Japan

ABSTRACT

In intermittent gas jets, the influence of gas injection conditions on ambient gas entrainment structure and processes were evaluated by a LIFA (laser-induced fluorescence of ambient gas) technique. The influence of injection nozzle diameter, D, the ratio of nozzle length to diameter, L/D, kinematic viscosity of the gas jet, ν, and discharge velocity, u_m, up to the velocity of sound were investigated. Experimental results show that the influence of injection conditions on the ambient gas entrainment processes correlates simply with the influence of eddy kinematic viscosity, ν_t, calculated from the discharge turbulence intensity of jets. The discharge turbulence intensity increases with an increase in u_m and with decreases both in L/D and nozzle diameter. The mean jet concentration, Cjm, which was calculated by averaging Cj over the whole jet and assuming that the jet is symmetric around the central axis, can be predicted approximately with only one parameter, $D^2/(\nu+\nu_t)\Delta t$.

INTRODUCTION

An understanding of the mixture formation processes in intermittent gas jets is important not only to improve the performance of DI gas engines but also to understand a Diesel spray. A number of gas jet investigations have dealt with the external features and structure of the jets [1-3].

A quantitative analysis calculating mixture strength, suffers from the difficulty of measuring instantaneous concentrations with sufficient accuracy and so is less studied. Until now, hot wire probes [4-5] and Rayleigh scattering techniques [6] have been applied to quantitative measurements and analysis. Other optical techniques have also been applied, incident light extinction [7] and holographic interferometry [8-9] for non-evaporating diesel spray, and Raman scattering for SI engines [10].

Recently, laser-induced fluorescence (LIF) has been applied in various areas: mixture formation in SI engines was investigated qualitatively by the fluorescence of NO_2 [11], the mole fractions of steady gas jets were measured with the fluorescence of iodine in the jet [12], the vapor and liquid concentrations in a Diesel spray were measured qualitatively with the exciplex technique [13-15].

To enable a quantitative concentration analysis of intermittent gas jets with sufficient accuracy, the authors developed a laser-induced fluorescence of ambient gas technique, LIFA[16], and applied it to quantify intermittent gas jets with various injection conditions to establish the general nature of ambient gas entrainment phenomena and structure in intermittent gas jets.

EXPERIMENTAL APPARATUS AND PROCEDURES

Figure 1 shows a plan of the optical arrangement of the LIFA and gas injection systems. Gas is injected intermittently into a box-shaped vessel with quarts windows. The "rectangular" type injection rate pattern was obtained by an injection nozzle with an electric valve. Discharge velocities of the gas jets were up to the velocity of sound, and were controlled by gas pressure. The nozzles used in the experiment had 0.6, 0.8, or 1 mm diameters, and had the ratios of nozzle length to diameter, L/D, 1, 5, 10, or 20 with each of the three nozzles. The gas jet was injected into the vessel at atmospheric pressure during injection, as the vessel is not sealed. Helium and argon were used as both jet and ambient gas.

Iodine was used as the fluorescence agent, and was mixed in the ambient gas. The iodine concentration was controlled by the temperature inside the vessel, and was kept at 333K. Iodine absorbs the second harmonic of Nd:YAG laser beams (532 nm) and emits relatively strong fluorescence. Laser light was expanded and thinned with two cylindrical lenses and a convex lens to create a 70 mm high and 0.3mm wide light sheet. The

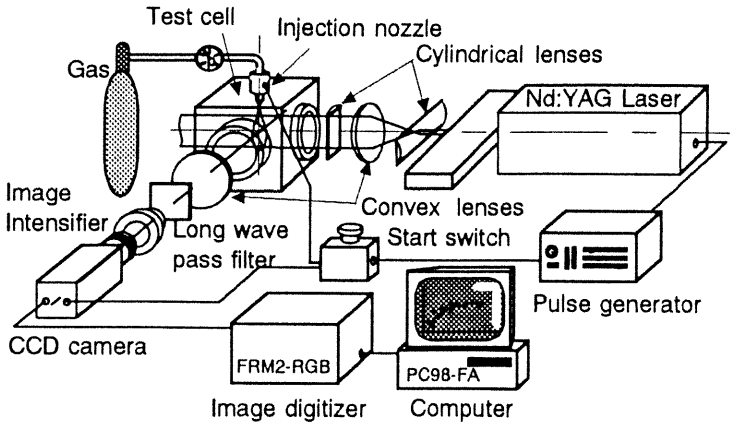

Fig.1 Plan of the LIFA system

maximum power of the Nd:YAG laser used in this study was 350 mJ/pulse.

The fluorescence in the ambient gas was amplified by an image intensifier, detected by a CCD camera and recorded by an image processor. To record only the fluorescence with high S/N ratios, a long wavelength pass filter was installed directly in front of the image intensifier. It transmits 10%, 50%, and 90% of incident light at 590, 600, and 630 nm respectively. The image processor had 256 gradations and 512×512 pixels.

Discharge velocities of intermittent gas jets for all kinds of nozzles tested here were measured with a hot wire anemometer, and discharge turbulence intensities were calculated as one of the injection parameters.

QUANTITATIVE ANALYSIS OF JET CONCENTRATIONS

When laser sheet light is inserted into the jet, as indicated in Fig.2, the fluorescence of the n-th calculation grid from inside the jet, F_n, measured at the plane parallel to the sheet light plane (y=0) is given by Lambert-Beer's law, as:

$$F_n = \Phi\ \alpha\ J_0 \exp\left(-k_x \Delta \sum_{m=1}^{n} C_{m-1}\right)\left[1-\exp(-k_x C_n \Delta)\right] \qquad (1)$$

where, $J_0 = J_s(1- \exp(-k_x C_0 L_x))$

$\alpha = \exp(-k_y C_0 L_y)$

J_s : Initial number of photons inserted into the vessel
Φ : Quantum yield
k_x : Absorption coefficient for the excitation wavelength
k_y : Absorption coefficient for the wavelength of observed fluorescence
C_0 : Initial concentration of fluorescence agent in the ambient gas
C_n : Concentration of fluorescence agent at the n-th calculation grid
Δ : Grid size
L_x : Laser light traveling distance
L_y : Distance between the sheet light plane and the observation window

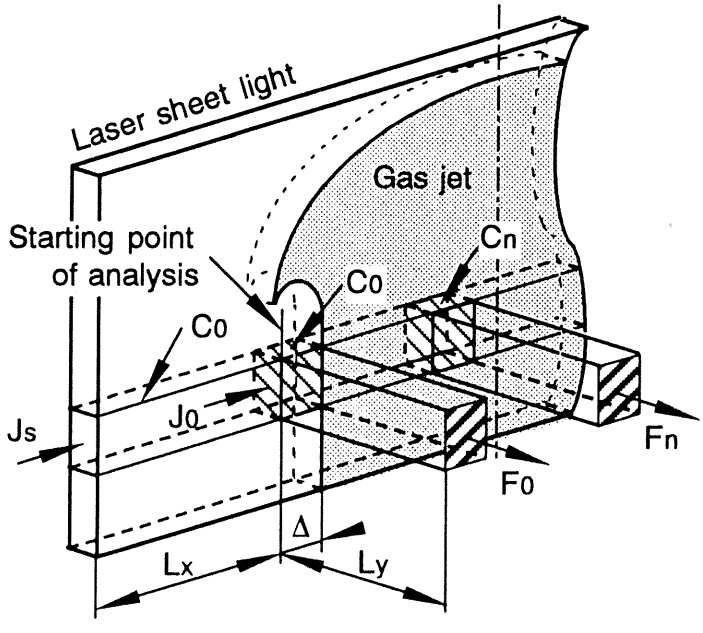

Fig.2 Model of the LIFA image analysis

Rearranging Eq. (1) gives Cn as:

$$C_n = \frac{-1}{k_x \Delta} \ln\left[1- \frac{F_n}{\Phi\alpha\ J_0} \exp\left(k_x \Delta \sum_{m=1}^{n} C_{m-1}\right)\right] \qquad (2)$$

When the image analysis starts from just the outside the jet, the constant $\Phi\alpha J_0$ is given by F_0. Thus the basic equation for this quantitative analysis becomes

$$C_n = \frac{-1}{k_x \Delta} \ln\left[1- \frac{F_n}{F_0} \beta \exp\left(k_x \Delta \sum_{m=1}^{n} C_{m-1}\right)\right] \qquad (3)$$

where, $\beta = 1- \exp(-k_x C_0 \Delta)$

It is notable that the concentration of the fluorescence agent, C_n, can be calculated from the measured fluorescence, F_n and F_0 without measuring the power of the laser sheet light.

Using the calculated concentration of the fluorescence agent, C_n, the volumetric concentration of the jet, Cj(n), is obtained by Eq. (4) when assuming constant pressure and temperature,

$$Cj(n) = 1-C_n/C_0 \qquad (4)$$

As a result, quantitative calculations of jet concentrations can be carried out with Eqs. (3) and (4).

EXPERIMENTAL RESULTS AND DISCUSSIONS

Influence of Discharge Velocity on Jet Concentration Distribution

Figure 3 shows the two dimensional concentration distribution of helium jets for three discharge velocities, u_m, the mean velocity during the injection. The images of jet concentrations show eight gradations of the volumetric concentration, Cj, and a 1mm diameter nozzle and L/D 5 was used.

The figure shows that the structure of the intermittent gas jets are quite different for the different discharge velocities. With increasing u_m, the radial expansion of the jets initially decreases, and then shows some increase. In high speed jets, the jet is broken up near the outlet of the nozzle and entrainment of ambient gas into the jet is enhanced. These phenomena are quite similar to those of a Diesel spray[17].

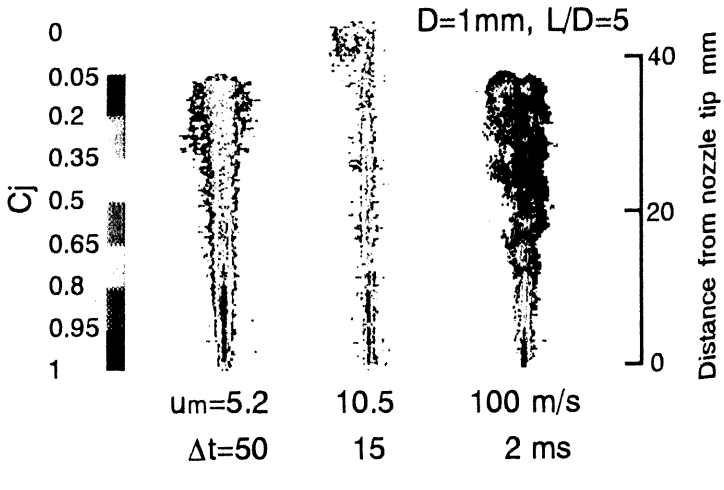

Fig.3 Sectional plane of jet concentrations on the jet center axis at different discharge velocities

Axial concentration profile. Axial concentration profiles along the center line of the jet in intermittent gas jets could be classified into steady and unsteady regions. Figure 4 shows the axial concentration, Cja, for low and high speed jets. In the figure, the broken curves indicate profiles of steady jets calculated with the following equation[18].

$$Cja = \frac{a}{z+b} \qquad (5)$$

Here, z is the axial distance from the nozzle tip, and a and b are constants. The curves for the steady region with each injection condition were set from measured values, using the least squares method.

With increasing axial distance from the nozzle tip Cja decreases, but in the unsteady region Cja decreases below the calculated Cja for steady jets and then shows a maximum near the top of the jet. It is notable that the maximum values of Cja are higher than those of the calculated Cja for steady jets. With increasing discharge velocity, both Cja and the length of the steady region decrease.

Length of steady region, Ls. Figure 5 shows the relation between Ls and u_m, for helium and argon jets growing to around 60mm in jet length, Ls shows a maximum, that is, Ls increases with increasing u_m and then decreases to approach a constant value asymptotically. A value of u_m which gives the maximum Ls is much lower for argon than for helium jets.

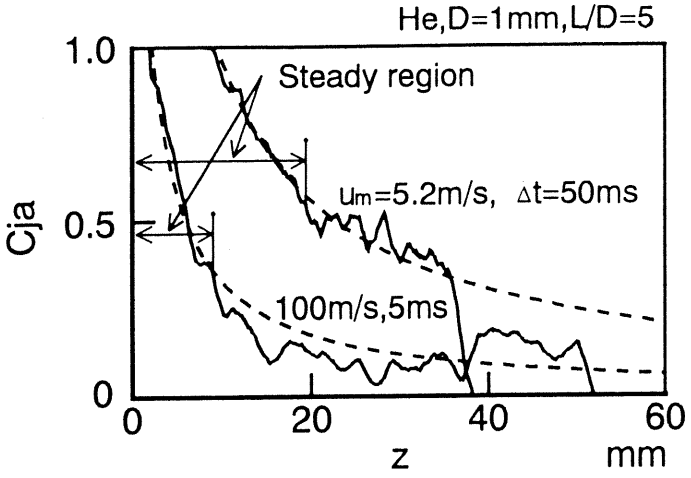

Fig.4 Axial jet concentration profiles along the jet center line

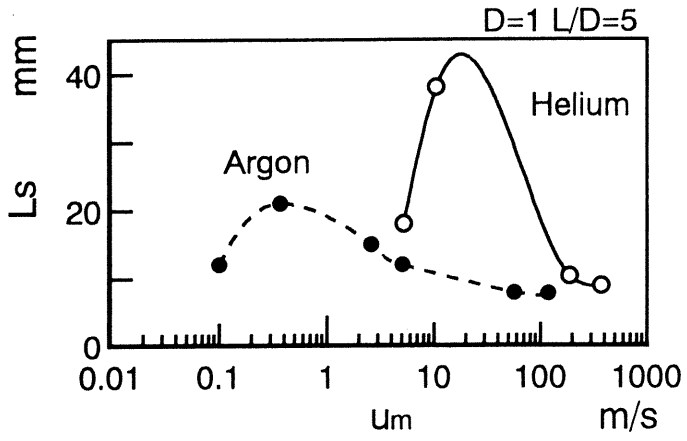

Fig.5 Relation between the length of the steady region, Ls, and discharge velocity, u_m

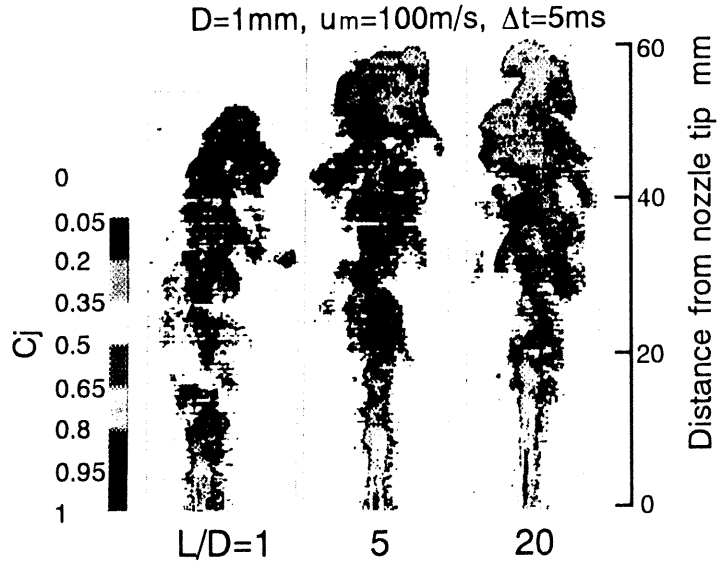

Fig.6 Sectional plane of jet concentrations on the jet center line for different L/D

Influence of L/D

Figure 6 shows the jet concentration distribution for helium jets for three L/D, here the nozzle diameters, the discharge velocities, and the time after the start of injection are all the same. With decreasing L/D, the length of the steady region decreases, the radial expansion of the jet and entrainment amount of ambient gas increase inversely. Complicated structures resembling a fir cone appears in the unsteady region of the jets.

Figure 7 shows the length of the steady region, Ls, for three L/D with the same nozzle diameter; Ls decreases with a decrease in L/D.

Figure 8 shows Cja profiles for the jets in Fig.6. This figure indicates that the entrainment of ambient gas into jets is much higher for lower L/D. In the unsteady region, Cja fluctuates both over large and small spatial scales. This phenomenon is due to the fir cone structure in the unsteady region of the jets.

Spectrum Analysis of Cja

The spectrum analysis of the fluctuation of Cja was based

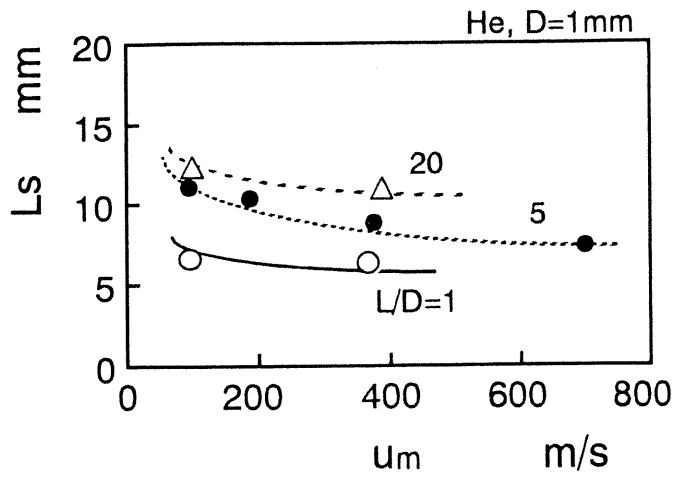

Fig.7 Length of the steady region in intermittent gas jets for different L/D

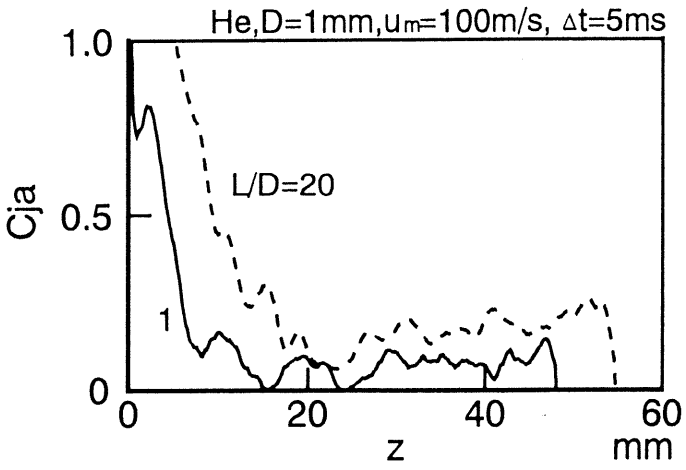

Fig.8 Axial jet concentration profiles for different L/D

on the Blackman-Turkey method[19]. The spectrum analysis in this study were spatial fluctuations of Cja in the jets, and the wave number was used instead of frequency for the calculation of power spectra.

Figure 9 shows the relation between wave number and densities of a one-sided power spectra. The wave number which gives the maximum density decreases with increases in elapsed time after the start of injection, Δt. This suggests that the major spatial scale of the entrainment gas flow in jets grows larger with lapse of time, Δt.

Figure 10 shows power spectra calculated from the data in Fig.8. Below a wave number of 0.1/mm, the peak density increases with increasing L/D, but above 0.1/mm, the density decreases with increasing L/D. This suggests that with decreasing L/D, the small spatial scale gas flow in jets increase.

Discharge Turbulence Intensity

In this study, discharge velocities were measured 0.2mm from the nozzle tip, and the turbulence intensities were calculated. Figure 11 shows the relation between mean discharge velocity, u_m, and mean turbulence intensity, u'_m. The values of u_m and u'_m are the averages during the injection period, u'_m increases with increasing u_m and decreasing L/D. The influence of u_m and L/D on u'_m is relatively smaller in argon jets than in helium jets.

Figure 12 shows u_m vs. u'_m for three nozzle diameters, u'_m increases with decreasing the nozzle diameter.

Overall, the influence of increased u'_m includes decreases in Ls and Cja with increasing u_m and decreasing L/D, and there is an increase in smaller spatial scale components in jets with decreasing L/D.

Relationship between Mean Jet Concentration and Injection Parameters

Figure 13 shows the time history of the mean jet concentration, Cjm, for 1mm diameter nozzles and a discharge velocity of 100m/s. The Cjm was calculated by averaging Cj over the whole jet assuming that the jet is symmetric around the central axis. The figure shows that Cjm decreases with time elapsed after injection, Δt, and also with lower L/D. Especially after 2 ms, here Cjm appears higher with argon jets of L/D=20, and lower with helium jets of L/D=1. This order is quite similar to that of the turbulence intensity in Fig.11, lower Cjm corresponds to the higher turbulence intensity.

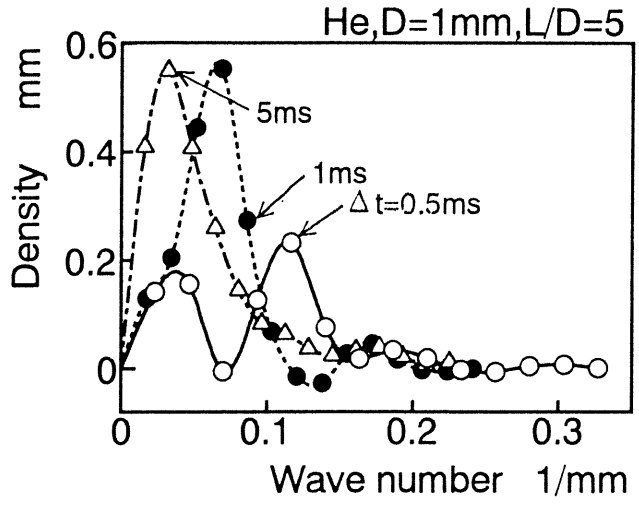

Fig.9 Power spectra of Cja at different times elapsed after the start of injection, Δt

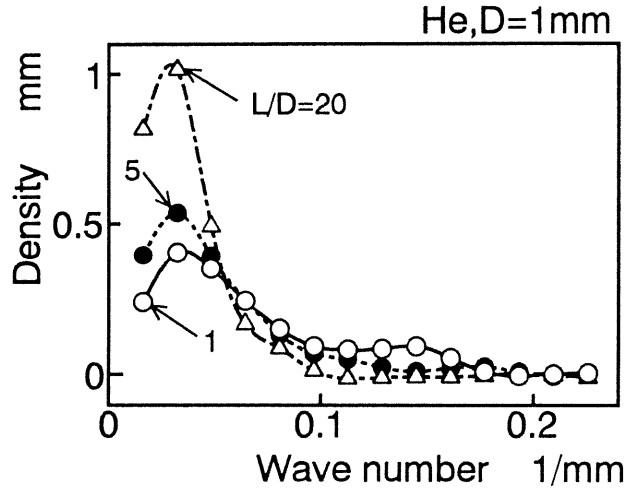

Fig.10 Power spectra of Cja at different L/D

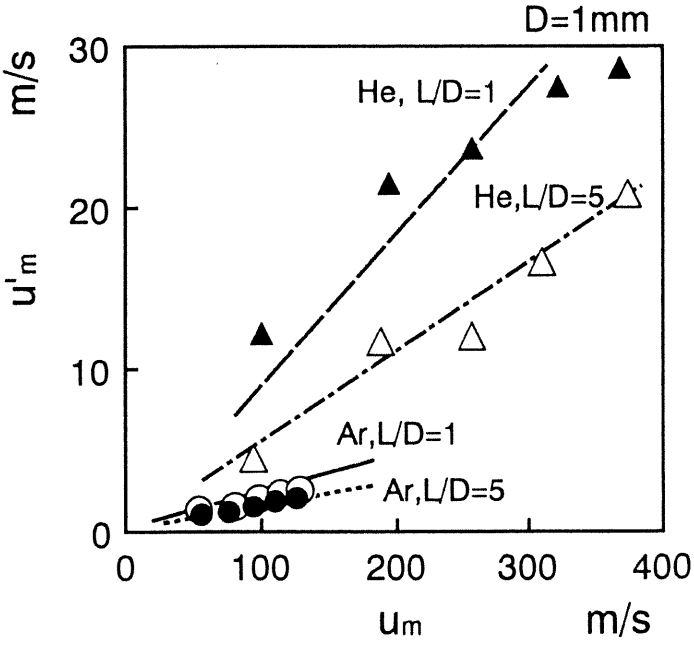

Fig.11 Relation between discharge turbulence intensity, u'_m, and discharge velocity, u_m, for various injection conditions

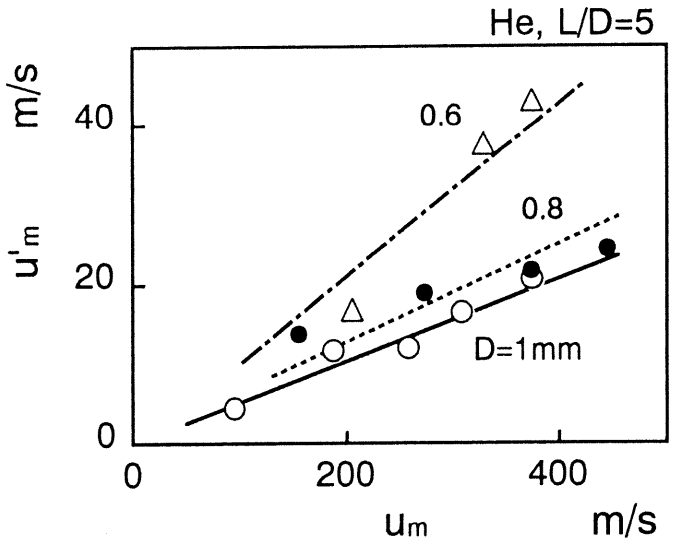

Fig.12 Discharge turbulence intensities for various nozzle diameters

According to the equation for steady jets reported by Öz[20], the velocity along the jet central axis, u_{max}, is expressed as:

$$\frac{u_{max}}{u_0} = A\frac{u_0 D^2}{\nu^* z} \qquad (6)$$

where, A is a constant, u_0 is the discharge velocity, ν^* an effective viscosity, and z is the axial distance from the nozzle tip.

The value of ν^* is given by a summation of ν and ν_t, where ν is a kinematic viscosity of the jets and ν_t an eddy kinematic viscosity. A ν_t is obtained by the assumption that the turbulence intensity is the same in all directions and that mixing length is equivalent to the nozzle diameter[21], as

$$\nu_t = C\sqrt{\frac{3}{2}}u'_m D \qquad (7)$$

where C is a constant.

As u_{max}/u_0 corresponds to Cja, the Cja of steady jets can be predicted by Eq.6. Assuming that Cjm and Cja correlate in this study, the following equation was obtained, rearranging Eq.6 by substituting $u_0\Delta t$ into z.

$$Cjm = f\left(\frac{D^2}{(\nu+\nu_t)\Delta t}\right) \qquad (8)$$

here, f is a function

The relationship between Cjm and the parameter, $D^2/(\nu+\nu_t)\Delta t$, was given as shown in Fig.14. The constant C is selected as 5.9. The Cjm in this figure correlates well with only one parameter independent of both the discharge velocity and the nozzle diameter and also the turbulence intensity and the jet property. This indicates that the nature of ambient gas entrainment into jets can be predicted with some of the injection conditions.

CONCLUSIONS

The influence of gas injection conditions on ambient gas entrainment processes was evaluated by a laser-induced fluorescence of ambient gas technique, LIFA.

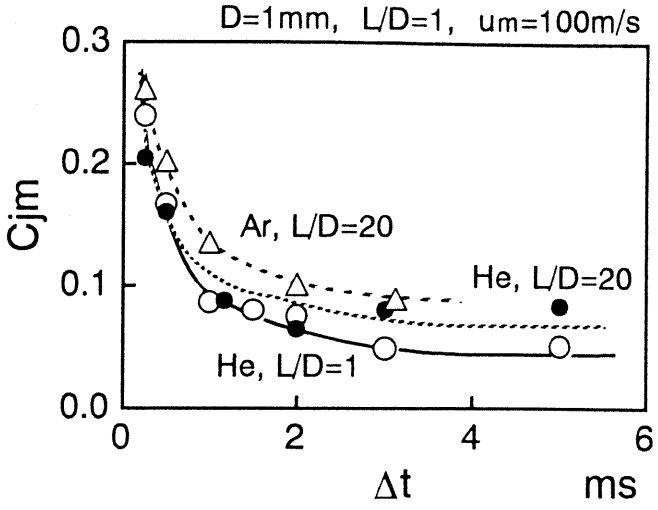

Fig.13 Time history of Cjm, mean jet concentrations.

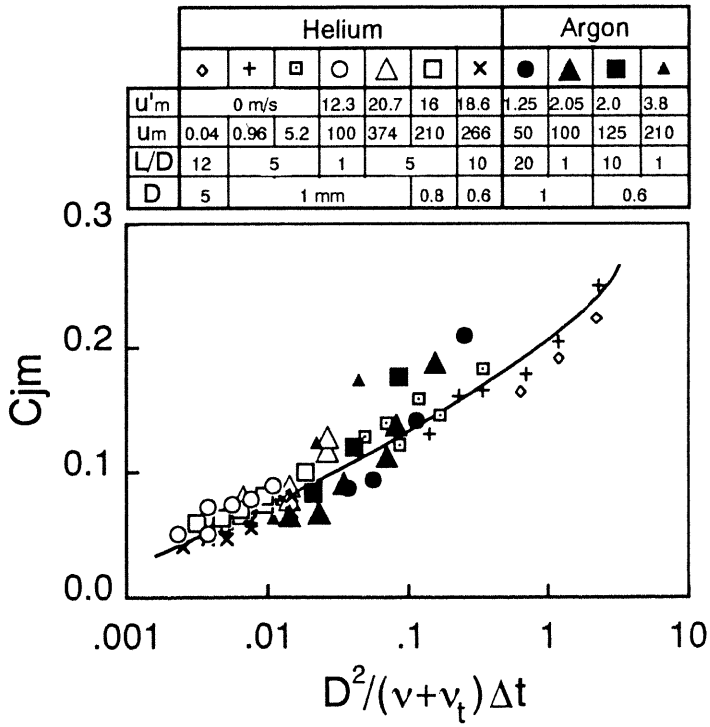

Fig.14 Relation between Cjm and the variable $D^2/(\nu+\nu_t)\Delta t$

The results of this investigation may be summarized as follows:

1. The mean jet concentration can be evaluated and predicted with only the parameter $D^2/(\nu+\nu_t)\Delta t$, where D is nozzle diameter, Δt the time elapsed after the start of injection, and ν_t the eddy kinematic viscosity calculated from u'_m.

2. The influence of injection conditions on the ambient gas entrainment processes in the intermittent gas jets correlates simply with the influence of the eddy kinematic viscosity or discharge turbulence intensity in jets.

3. Discharge turbulence intensity increases with increase in discharge velocity, u_m, and decreases in both L/D and nozzle diameter. These results explain the decrease in axial length of

the steady region and Cja with increasing u_m and decreasing L/D, and the increase in small entrainment scale components with decreasing L/D.

4. The spatial scale of gas flow in jets grows larger with lapse of time, and small scale components increase with decreasing L/D.

5. The axial jet concentration, Cja, peaks near the tip of the jet, and fluctuates with the spatial scale, corresponding to a fir cone structure in high speed jets.

ACKNOWLEDGMENT

The authors wish to express their appreciation to Ms. M. Katayama and Mr. M. Ueno, graduate and undergraduate students of Hokkaido University for their cooperation in the experiments in this investigation.

REFERENCES

[1] Witze, P. O., "Hot-Film Anemometer Measurements in a Starting Turbulent Jet," AIAA J., Vol.21, No.2, p.308, 1983.

[2] Ricou, F. P., and Spalding, D. B., "Measurement of Entrainment by Axisymmetrical Turbulent Jets," J. Fluid Mech., vol.11, p.21, 1961.

[3] Long, M. B., Chu, B. T., and Chang, R. K., "Instantaneous Two-Dimensional Gas Concentration Measurements by Light Scattering," AIAA J., Vol.19, No.9, p. 1151, 1981.

[4] Iida, N., Hirano, K., and Sato, G. T., "Experimental Study of Transient Gas Jet Impinging on a Wall," SAE Trans. Vol.99, Sec.3, Paper No.900479, pp.1090-1100, 1990.

[5] Tanabe, H., Suzuki, N., Sorihashi, T., Fujimoto, H., and Sato, G. T., "Experimental Study on Transient Gas Jet," Proc. 19th Int. FISITA Congress, 82026, 1982.

[6] Arcoumanis, C., Green, H. G., and Whitelaw, J. H., "The Application of Laser Rayleigh Scattering to a Reciprocating Model Engine," SAE Trans. Vol.93, Sec.2, Paper No.840376, pp.949-959, 1984.

[7] Kamimoto, T., Ahn, S. K., Chang, Y. J., Kobayashi, H., and Matsuoka, S., "Measurement of Droplet Diameter and Fuel Concentration in a Non-Evaporating Diesel Spray by means of an Image Analysis of Shadow Photographs," SAE Trans. Vol.93, Sec.2, Paper No.840276, pp.372-380, 1984.

[8] Dent, J. C., Keightley, J. K., and De Boer, C. D., "The Application of Interferometry to Air Fuel Ratio Measurement in Quiescent Chamber Diesel Engine," SAE Trans. Vol.86, Sec.4, Paper No.770825, pp.2858-2869, 1977.

[9] Nishida, K., Murakami, N. and Hiroyasu, H., "A Pulsed-Laser Holography Study of the Evaporating Diesel Spray in a High Pressure Bomb," Preprint of COMODIA-85, p.141, 1985.

[10] Smith, J. R., "Temperature and Density Measurements in a SI Engine by Pulsed Raman Spectroscopy," SAE Trans. Vol.89, Sec.1, Paper No.800137, pp.808-816, 1980.

[11] Cole, J. B., and Swords, M. D., "Measurement of Concentration Fluctuations in an Internal Combustion Engine," Apply Physics, Vol.13, pp.733-745, 1980.

[12] Hollo, S. D., Hartfield, R. J. Jr., and McDaniel J. C., "Injectant Mole Fraction Measurements of Transverse Injection in Constant Area Supersonic Ducts," AIAA 90- 1632, 1990.

[13] Melton L. A., and Verdick, J. F., "Vapor/Liquid Visualization in Fuel Sprays," Preprint of 20th Symposium on Combustion, pp.1283-1290, 1984.

[14] Bardsley, M. E. A., Felton, P. G., and Bracco, F. V., "2-D Visualization of Liquid and Vapor Fuel in an I. C. Engine," SAE Trans. Vol.97, Sec.3, Paper No.880521, pp.281-291, 1988.

[15] Senda, J., Fukami, Y., Tanabe, Y., and Fujimoto, H., "Visualization of Evaporative Diesel Spray Impinging upon Wall Surface by Exciplex Fluorescence Method," SAE Trans. Vol.101, Sec.3, Paper No.920578, pp.1054-1063, 1992.

[16] Kido, A., Ogawa, H., and Miyamoto, N., "Quantitative Measurements and Analysis of Ambient Gas Entrainment into Intermittent Gas Jets by Laser-Induced Fluorescence of Ambient Gas (LIFA)," SAE Paper No. 930970, pp.1-9, 1993.

[17] Arai, M., Tabata, M., Hiroyasu, H., and Shimizu, M., "Disintegrating Process and Spray Characterization of Fuel Jet Injected by a Diesel Nozzle," SAE Trans. Vol.93, Sec.2, Paper No.840275, pp.358-371, 1984.

[18] Abramovich, G., N., The Theory of Turbulent Jets, M.I.T. Press, pp.89-102, 1963.

[19] Hino, M., Spectrum Analysis, Asakura-shoten, Japan, pp.184-193, 1977. (in Japanese)

[20] Öz, I. H., "Calculation of Spray Penetration in Diesel Engines," SAE Trans. Vol.78, Sec.2, Paper No.690254, pp.1107-1116, 1969.

[21] Japan Society of Mechanical Engineering, Numerical Flow Simulation, Corona-sha, Japan, pp.265-281., 1988. (in Japanese)